INFLUENCE OF COOLING ON THE PHASES DEVELOPMENT IN INDUSTRIAL SÍNTER[1]

Soledad Oreggioni[2]
Silvina Ramos[2]
Pedro Etchevarne[3]
Ariel Rapetto[3]

Abstract

The demands on sinter quality are increasing due to the tendency to charge more sinter in the blast furnace burden. For this reason, it is highly important the knowledge about the influence of the chemical composition and the structure on sinter quality. When is being manufactured at industrial level, after the sinter leave the strand, it begins a series of steps designed to adjust the size distribution and cool the sinter before charging to the blast furnace. This cooling and the formed phases have a big importance on the quality of the sinter such as mechanical strength, reducibility and reduction degradation. The objective of this study is to evaluate the influence of cooling used at an industrial level on formed phases in the microstructure of sinter. Samples extracted from plants with different cooling conditions were studied applying chemical analysis, electronic and optical microscopy and X-ray diffraction.

Key words: Sinter; Cooling; Microstructure

INFLUÊNCIA DO MÉTODO DO RESFRIAMENTO SOBRE O DESENVOLVIMENTO DO FASES EM SINTER INDUSTRIAL

Resumo

As exigências sobre a qualidade do sinter estão a aumentar devido a uma tendência de aumentar as proporçoes de carga no alto forno. Por esta razão é extremamente importante aumentar o conhecimento sobre a influência da composição química e da estrutura sobre o comportamento da sinterização. Quando a produção industrial, após o sinter tem atravessado a cadeia de sinterização, começa uma série de medidas destinadas a ajustar o tamanho e arrefecer o sinter de carga no alto-forno. Este arrefecimento e as suas condições são de grande importância para a qualidade do sinter como eles definem as fases formadas no interior da qualidade e parâmetros tais como resistência mecânica, reducibility e degradação através da redução. O objetivo deste estudo é avaliar a influência de resfriamento usado em um nível industrial formada por fases na microestrutura da sinterização. As amostras extraídas de plantas com diferentes condições resfriamento foram estudadas aplicando análise química, electrónica e de microscopia óptica e difração de raios X

Palavras-chave: Sinter; Resfriamento; Microestrutura.

---

[1] *Technical contribution to the 3rd International Meeting on Ironmaking, September 22 – 26, 2008, São Luís City – Maranhão State – Brazil*

[2] *Process Assistant, Ironmaking Area, IAS (Argentine Iron and Steel Institute), San Nicolás, Argentina.*

[3] *Process Engineer, Raw materials Area, Ternium Siderar, San Nicolás, Argentina.*

1 INTRODUCTION

The behavior of sinter in the blast furnace is determined by its quality. For this reason, increase the knowledge about the internal structure is relevant. This report presents a study about four samples taken at different stages of the process with different cooling conditions.

The mechanical strength of sinter is linked to the phases present in the sinter microstructure. These phases are usually: hematite, magnetite and calcium ferrite containing other elements such as aluminum and silicon. The calcium silicate results from the reaction of the different components of the mineral blend with fluxes and impurities introduced by the coke, which is incorporated into the mix as solid fuel. These components form a heterogeneous microstructure, associating phases in their original state or formed during the cooling of the mixture.

The physical, chemical and metallurgical properties of sinter, required for loading into the blast furnace, are influenced by the type of phases formed. Therefore the objective of this study is to identify the phases formed in different cooling conditions and make a qualitative comparison between the samples studied.

Ternium Siderar produces 2.8 Mt of steel slabs annually, the route of the process is blast furnace-oxygen steelmaking and continuous casting; it is the main steelmaking producer in Argentina and the only one making flat products in this country. They have two blast furnaces which are loaded with 30 percentage of sinter. The sinter plant has a productivity of 54 tn/m$_2$day with 81.2 m^2 of suction surface.

The Argentine Iron and Steel Institute- IAS- is a non-profit organization that comprises the main steel companies in Argentina, and it aims to carry out technological developments, as well as to provide technical assistance, analysis and testing to those companies.

2 MATERIALS AND METHODS

Four samples of sinter were studied, which were extracted at different points of the process and were left to cool to room temperature before being analyzed. They have different speeds of cooling, because of water addition on the production line and the process of air cooling. Table 1 and Figure 1 describe where the samples were extracted and their identification. Cooling speed of sample A< sample B< sample C.

Table 1. Sampling points and identification.

Identification	Sampling points
A	Extracted from the conveyor belt before the cooling process
B	Extracted at the middle of the cooling process
C	Extracted from the conveyor belt after the cooling process
D	Sample to be loaded at blast furnace

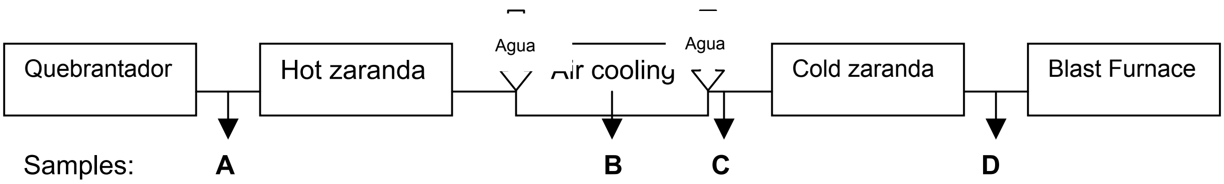

Figure 1. Sampling points.

All samples were studied by chemical analysis, X-ray diffraction and observation through optical and electronic microscope to identify the phases present, their morphological aspects and semi-quantitative composition.

3 RESULTS

3.1 Chemical Compositions

Table 2 shows the chemical compositions of the samples.

Table 2. Chemical compositions.

Composition (%)	Sample A	Sample B	Sample C	Sample D
Fe total	54,8	55,4	55,7	54,4
FeO	6,1	13,1	11,3	11,8
CaO	10,4	11,1	11,2	11,3
SiO_2	4,8	5,0	4,9	4,9
Al_2O_3	1,4	1,4	1,4	1,4
MgO	2,1	2,2	2,5	2,2
TiO_2	0,095	0,093	0,090	0,087

3.2 X-ray Diffraction

The crystalline phases present in each sample were identified by X-ray diffraction and were estimated the percentage by comparing qualitatively. The crystalline phases present were: hematite, magnetite, iron and calcium silicate and calcium ferrite.

In sample A 4 phases were identified: hematite, magnetite, iron and calcium silicate and calcium ferrite. The corresponding difractogram is presented in Figure 2.

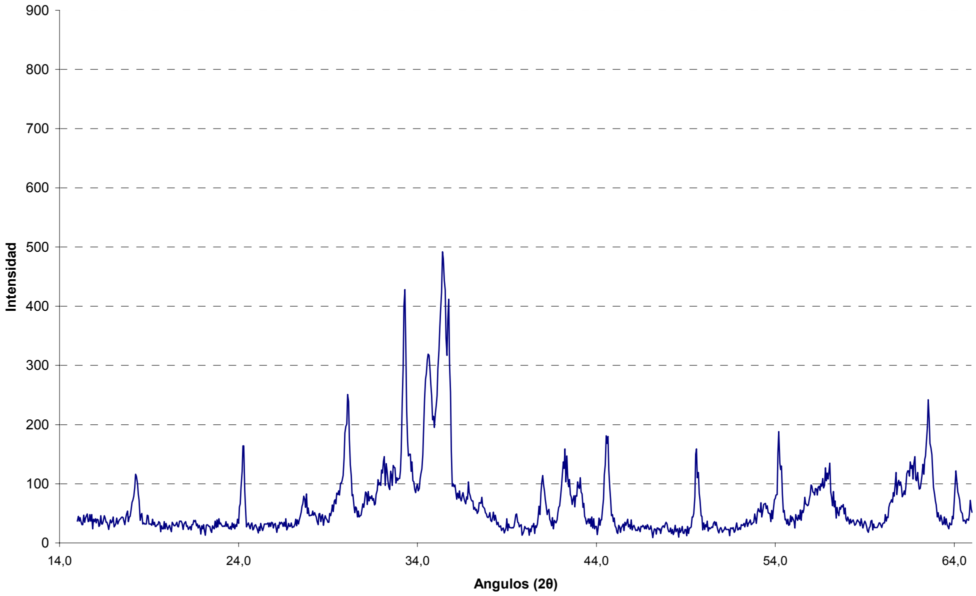

Figure 2. Difractogram of sample A.

In sample B we can see higher quantity of magnetite phase and lower quantity of hematite and calcium ferrite phases than sample A. The corresponding difractogram is presented in Figure 3.

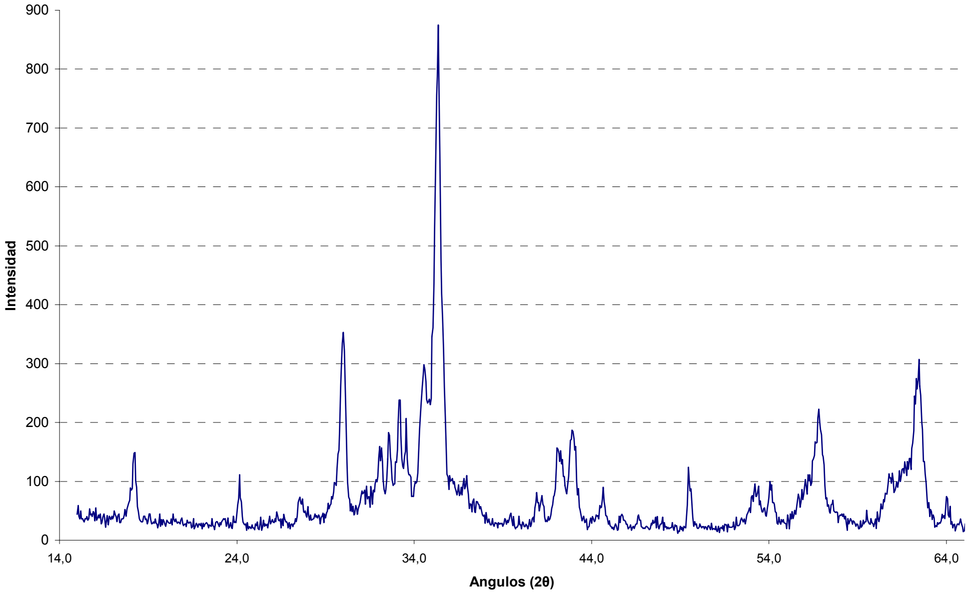

Figure 3. Difractogram of sample B

In sample C we can see lower quantity of magnetite phase and higher quantity of hematite and calcium ferrite phases than sample B. The corresponding difractogram is presented in Figure 4.

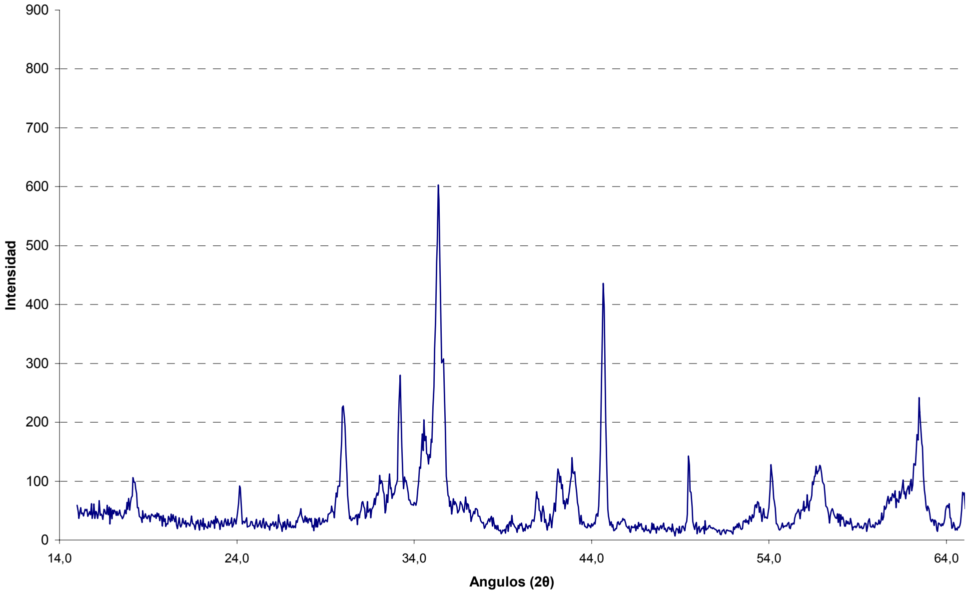

Figure 4. Difractogram of sample C

Sample D is very similar to sample C. Only we can observe lower quantity of calcium ferrite phase. The corresponding difractogram is presented in Figure 5.

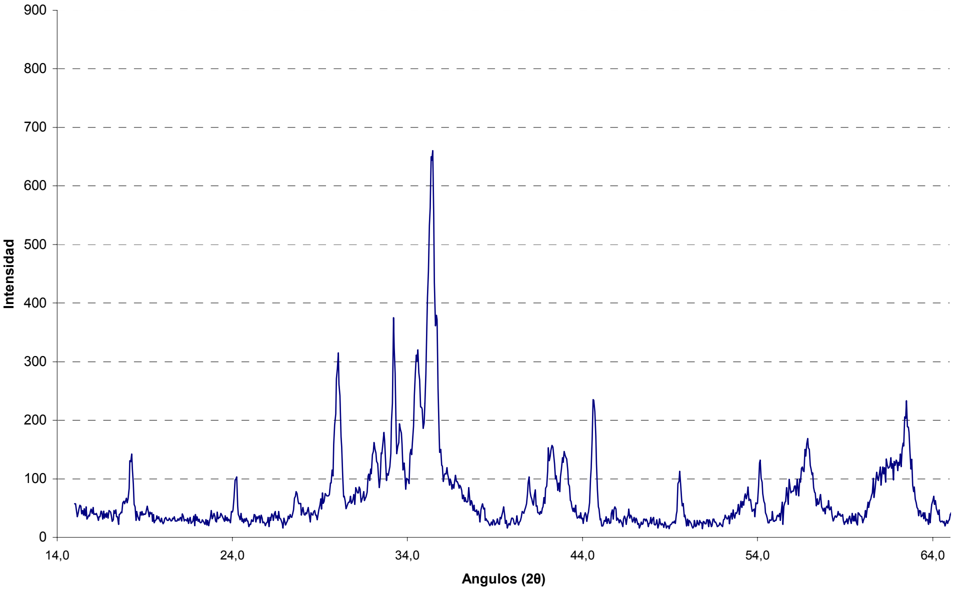

Figure 5. Difractogram of sample D

3.3 Microstructural Study

All samples were observed using optical and electronic microscope to evaluate the morphology and compositions of the phases present in the sinter structure.

The structure of sample A is made up of crystals of microporous hematite, white and polygonal (H), magnetite (M) and calcium ferrite (FC) (Figure 6). Elsewhere, hematite is presents as white phase with round edges (Figure 7). There is also magnetite (dark grey area) and initial formation of ferrite calcium.

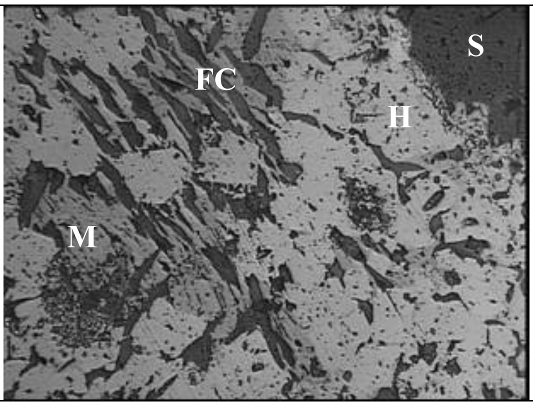	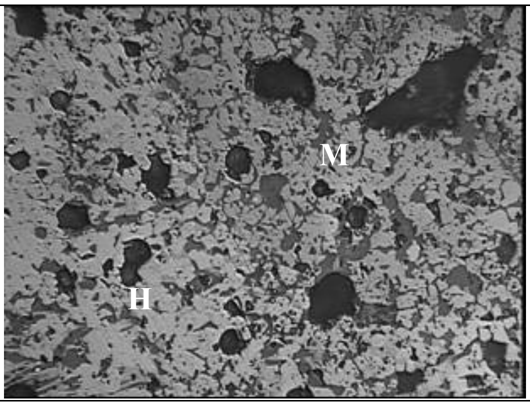
Figure 6. General structure of sample A. [M 256X]	**Figure 7.** Phases with round edges. [M 256X]

Using electronic microscopy we can identify hematite, calcium silicate and calcium ferrite with high silicon (Figure 8).

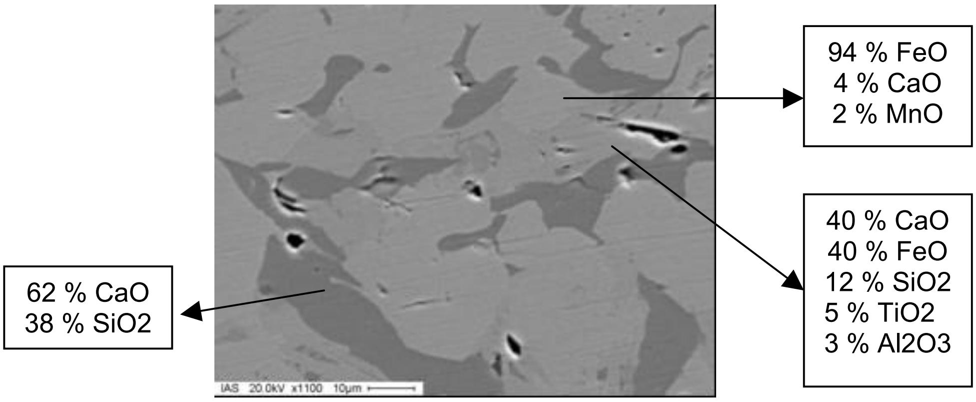

Figure 8. Hematite, calcium silicate and calcium ferrite [M 1100X]

The EDS analysis revealed the distribution of elements (Figure 9).

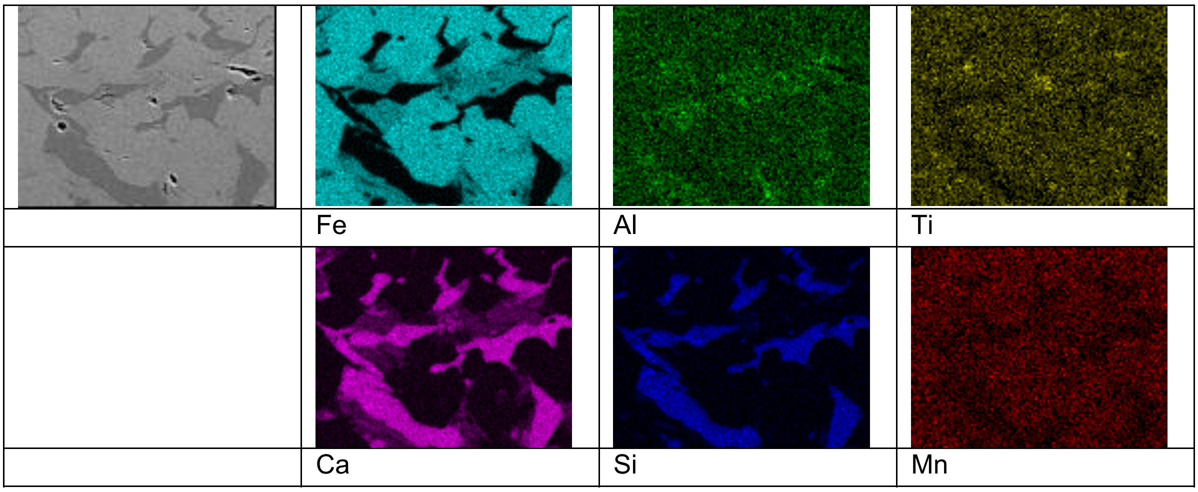

Figure 9. Elements identified: Fe, Al, Ti, Ca, Si y Mn

In another part of the sample, calcium ferrite with aluminum and silicon acicular morphology are distinguished, which are formed from the ferrous phase (phase gray clear) and acquiring development. The dark grey phase which is among the needles ferrite was identified as an iron and calcium silicate (Figure 10).

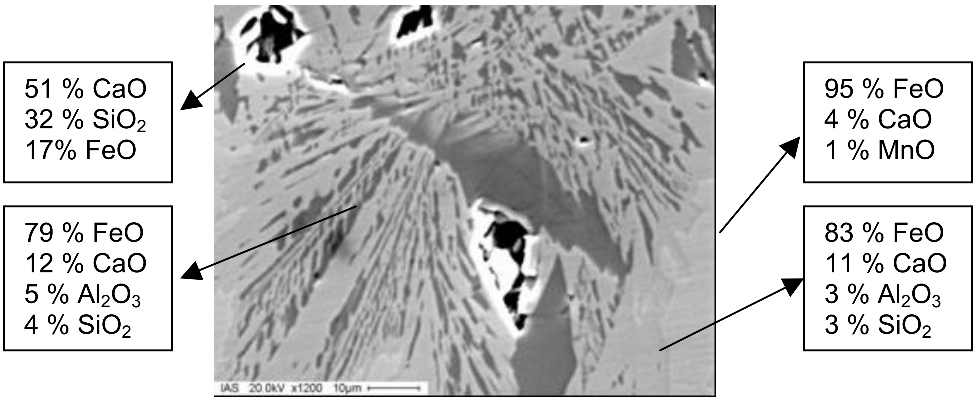

Figura 10. Acicular calcium ferrite [M 1200X]

Sample B structure presents acicular massive morphology (Figure 11). Only in localized areas of the sample is observed developments hematite with round edges (Figure 9).

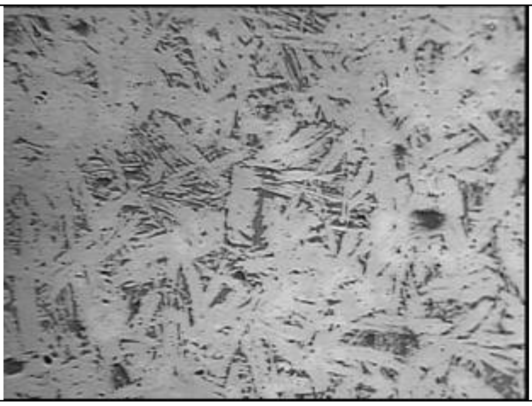	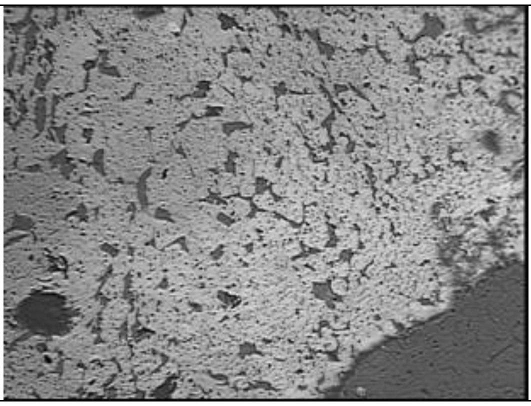
Figure 11. General structure of sample B. [M 256X]	Figure 12. **Phases with round edges.** [M 256X]

Through electronic microscopy we can observe hematite surrounded by dendrite calcium ferrite structure and calcium silicate phase (Figure 13).

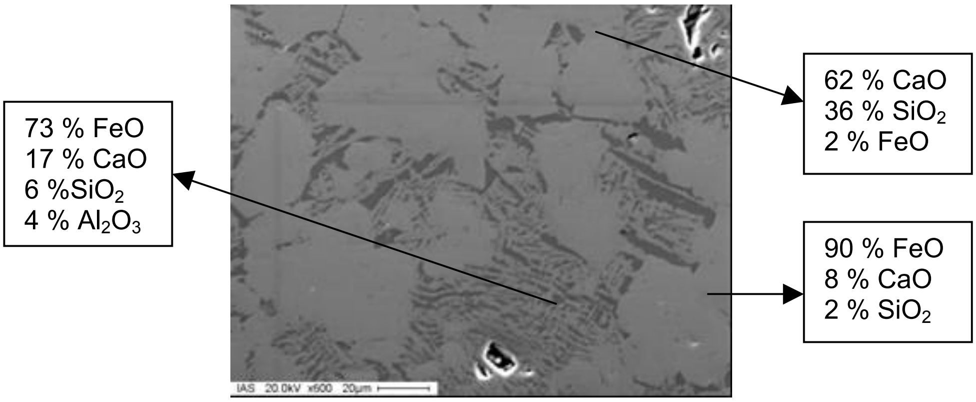

Figure 13. Hematite surrounded by dendrite calcium ferrite structure and calcium silicate phase [M 600X].

Elsewhere the sample is dominated by calcium ferrite type thick acicular (Figure 14).

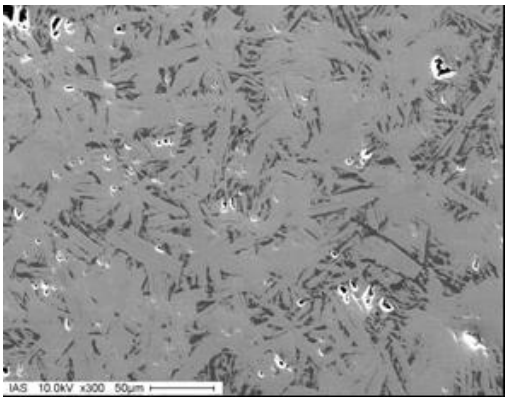

Figure 14. Calcium ferrite type thick acicular [M 300X].

Sample C structure is formed by microporous white hematite surrounded by a dendrite phase (Figure 15). In Figure 16 is observed secondary hematite crystals little porous and polygonal surrounded by acicular and dendrite ferrite phases.

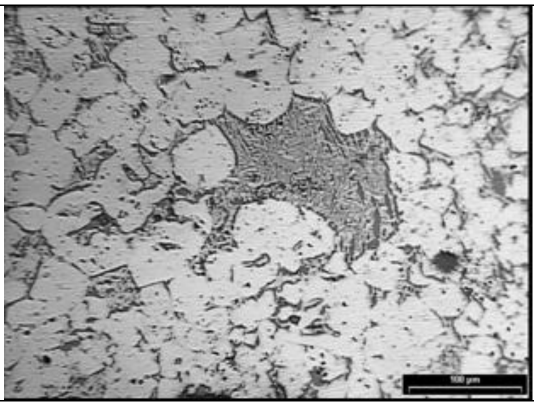

Figure 15. General structure of sample C. [M 256X]

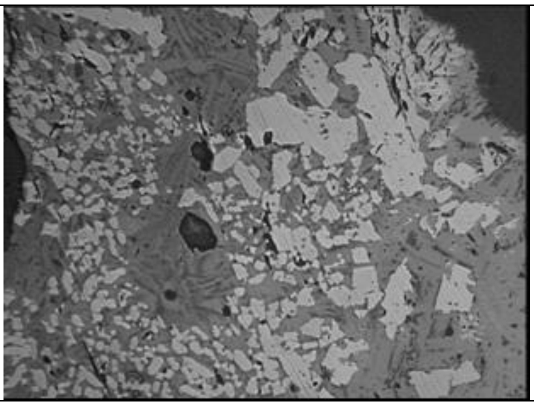

Figure 16. Secondary hematite crystals surrounded by ferrite phase [M 256X]

In another part of the sample high development of the acicular structure is observed (Figure 17)

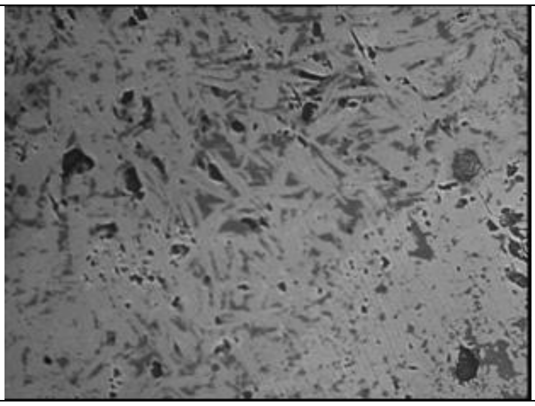

Figure 17. High development of the acicular structure. [M 256X]

The EDS analysis allows to identify dendrite structure formed by calcium ferrite with aluminum, silicon and magnesium and calcium silicate (Figure 18).

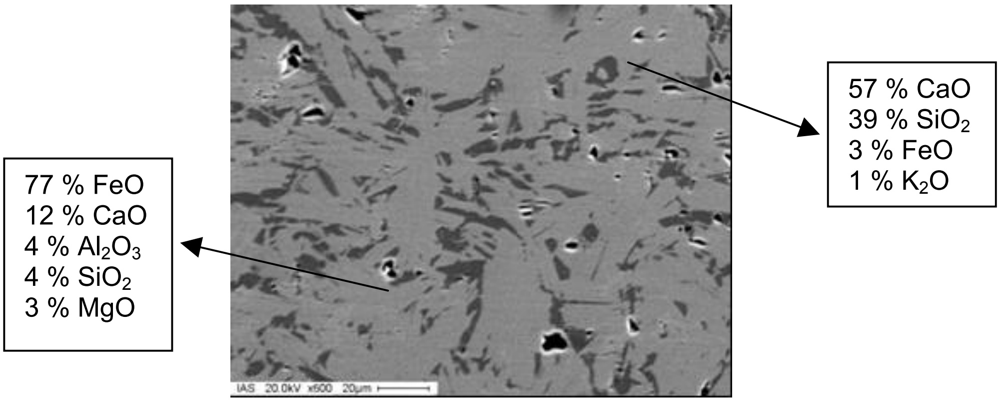

57 % CaO
39 % SiO_2
3 % FeO
1 % K_2O

77 % FeO
12 % CaO
4 % Al_2O_3
4 % SiO_2
3 % MgO

Figure 18. Calcium ferrite with aluminum and silicon. [M 600X]

In Figure 19 SFCA with different compositions inside a silicate matrix are observed.

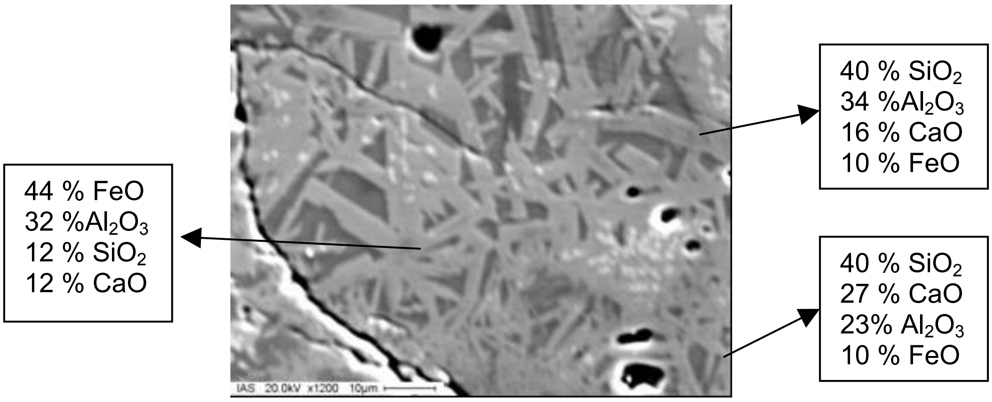

Figure 19. SFCA with different compositions inside a silicate matrix [M 1200X]

General structure of sample D presents magnetite phase with round edges, poor area with hematite and dendrite ferrite poorly developed (Figure 20). In the proximity of the pores polygonal crystals are observed that correspond to well-developed secondary hematite (Figure 21).

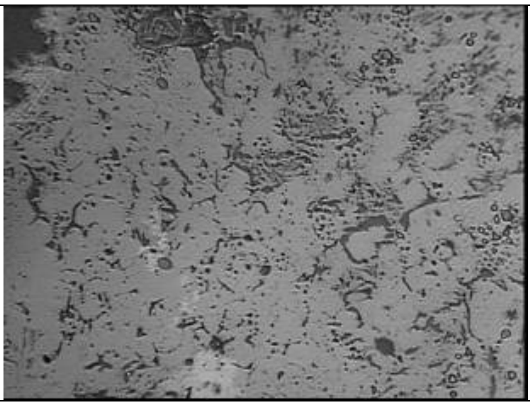	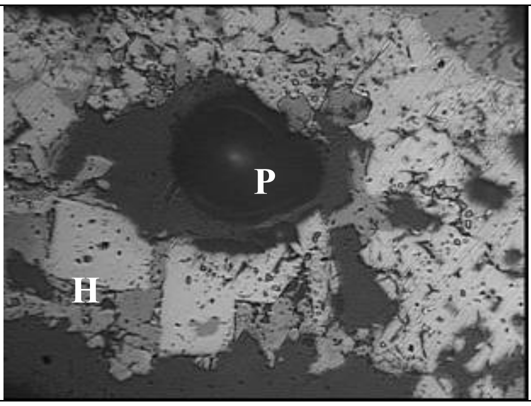
Figure 20. General structure of sample D. [M 256X]	**Figure 21.** Secondary hematite surrounding the pore [M 256X]

Also, there are areas where it dominates the acicular phase (Figure 22) and others with incipient formation of secondary hematite (Figure 23).

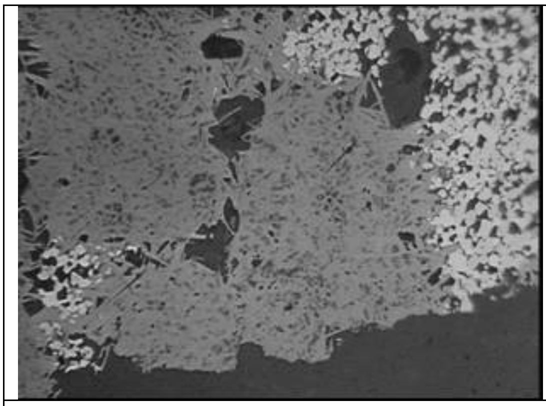	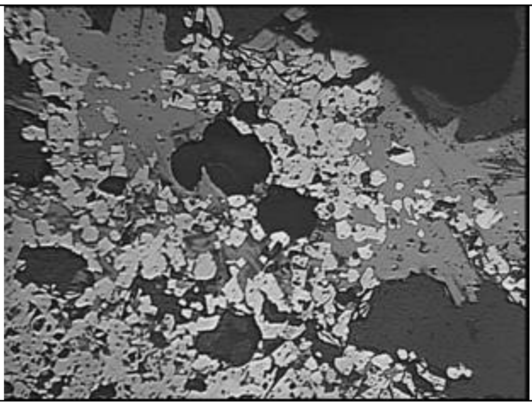
Figura 22. Areas where it dominates the acicular phase [M 256X]	**Figura 23**. Formation of secondary hematite [M 256X]

Electronic microscopy allows to identify that the acicular structure is formed by calcium ferrite with aluminum and silicon (Figure 24)

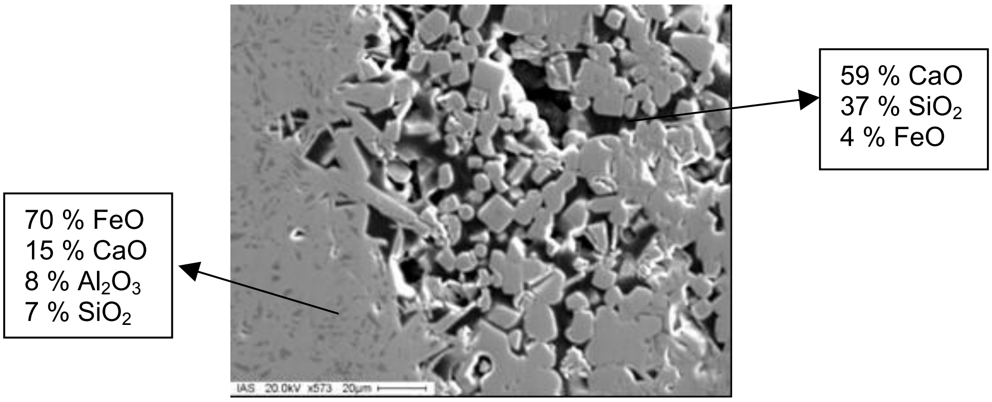

Figure 24. Calcium ferrite phase surrounding by calcium silicate phase. [M 573X]

4 DISCUSSIONS

The sinter mineralogy depends mainly on the mineralogical and chemical characteristics of the mixture, as well as the maximum temperature of the process, as long as it remains at that maximum temperature, and the cooling rate.

To understand the phases found in every cooling condition, it should take into account the reactions that happen at this stage. Melt formed during the sintering reaction has received ions Fe^{2+} and Fe^{3+} which are in a saturation state and precipitate forming hematite or magnetite phase or both while the melt is oxidized by air forming secondary hematite. The next step depends on basicity index and the cooling rate in the melt. According to the calcium content, other precipitation may occur after the hematite and magnetite, forming calcium ferrite. For basicity above 2.0, increases the proportion of calcium ferrite in the union of grains and reduces the proportion of calcium silicate. Considering the chemical analysis of samples the binary basicity is 2,23, so calcium ferrite phase forms part of the structure of the samples studied.

It was observed a great variation in the FeO percentage. The low-FeO is regarded as a good reducibility index because the FeO reacts with SiO_2 to form fayalite that is a difficult reduction phase.

During the sintering a molten material of calcium ferrite ($Fe_2O_3.CaO$) is formed containing small quantities of SiO_2 and Al_2O_3 that produces breaks in the interface of hematite nucleus that not melt. This situation improves the reducibility index. In that interface solid-liquid reactions are developed generating a network of acicular calcium ferrite with presence of SiO_2 and Al_2O_3 in the molten material. These SFCA are beneficial components in the structure of sinter as they have good reducibility and provide mechanical strength.

When it is sintered to low temperature the formation of magnetite is reduced (lower content of FeO) and the sinter improves its reducibility and its reduction degradation index (RDI). That is, when the sintering temperature is below 1300 º C provides a structure for optimal reducibility of sinter in the blast furnace, which is formed by a core of hematite (without melt) surrounded by acicular calcium ferrite. This structure presents the disadvantage of less physical resistance, so SiO_2 materials are added to the mix to increase the resistance.

The X-ray diffraction and microscopy allow to identify the crystalline phases in the samples.

Table 3. Phases identified in different samples.

Samples	Cooling conditions	Fases	Observations
A	Extracted before the air cooling process without water addition	• Little development of calcium ferrite • Microporous hematite • Hematite with edges rounds • Magnetite with edges rounds	It shows only a small amount of calcium ferrite not allowing greater development because of a high cooling rate
B	Extracted at the middle of the air cooling process with one water addition	• More development of acicular calcium ferrite • Dendritic calcium ferrite • Microporous hematite • A lot of magnetite	It shows more development of the acicular calcium ferrite phase. Also, the high magnetite content shows that the hematite reducing stage was favored and besides very little amount of calcium ferrite was generated.
C	Extracted from the conveyor belt after the air cooling process with two water additions	• Much acicular calcium ferrite • Dendritic calcium ferrite • Microporous hematite • Less magnetite • Formation of secondary hematite	Conditions allow generating greater quantity of calcium ferrite but also were formed secondary hematite from the oxidation of the magnetite
D	Sample to be loaded at blast furnace. Same cooling conditions to sample C.	• Acicular calcium ferrite • Dendritic calcium ferrite • Microporous hematite • Magnetite with edges rounds • Secondary hematite	No significant changes in its structure were presented with respect to the previous one.

So, sample B (extracted at the middle of the cooler with one water addition) presents an optimal structure which is formed by a core of hematite (without melt) surrounded by acicular calcium ferrite. However DRX analyses show high quantity of magnetite that affects the sinter reducibility and the reduction degradation index. Sample C (extracted after air cooling and two water additions) also presents the optimal structure but was formed secondary hematite from the oxidation of magnetite because of the cooling air and the water addition. This phase affects more the sinter reducibility and the reduction degradation index than the magnetite phase.

5 CONCLUSIONS

In this study it was possible to correlate the results obtained in each sample through chemical analysis and DRX with phases observed and identified using optical and electronic microscopy.

The ferrite calcium phase, which defines good quality parameters sinter, was identified in great proportion in the sample C, post-cooler, which could mean that the decline less severe temperature could favor the development of that stage. However, secondary hematite which was also identified is harmful to the sinter structure.

REFERENCES

1 W. KOWALSKI, K. KERSTING, The influence of sinter composition on sintering rate and physical quality of sinter, *1997 Ironmaking conference proceedings*, pp 415-424.

2 LI-HENG HSIEH y J.A. WHITEMAN, Sintering conditions for simulating the formation of mineral phases in industrial iron ore sinter, *ISIJ International,* Vol. 29 (1989), Nº 1, pp 24-32.

3 G.O. EGUNDEBI y J.A. WHITEMAN, Evolution of microstructure in iron ore sinters, *Ironmaking and steelmaking*, Vol. 16 (1989), Nº 6, pp 379-385

4 M. K. CHOUNDHARY, Evolution of sinter structure along bed height of quenched test pot, *ISIJ International*, Vol. 47 (2007), Nº 3, pp 516-518.

5 A. FORMOSO, A. MORO, Estudio de la granulación de la mezcla de minerales de hierro en el proceso de sinterización. I parte. Granulación*, Rev. Metal. Madrid 36 (2000)* pp 244-253.

6 H.P. PIMENTA y V. SESHADRI, Characterization of structure of iron ore sinter and its behavior during reduction at low temperatures, *Ironmaking and steelmaking*, Vol. 29 (2002), Nº 3, pp 169-174.